

## Ultrasonic resonator energy loss determination (chemical kinetics study)

This content has been downloaded from IOPscience. Please scroll down to see the full text.

1990 Meas. Sci. Technol. 1 385

(<http://iopscience.iop.org/0957-0233/1/5/002>)

View [the table of contents for this issue](#), or go to the [journal homepage](#) for more

Download details:

IP Address: 134.76.223.157

This content was downloaded on 04/01/2017 at 14:34

Please note that [terms and conditions apply](#).

You may also be interested in:

[New plano-concave ultrasonic resonator cells for absorption and velocity measurements in liquids below 1 MHz](#)

F Eggers, U Kaatze, K H Richmann et al.

[Ultrasonic spectroscopy of liquids. Extending the frequency range of the variable sample length pulse technique](#)

U Kaatze, V Kuhnel, K Menzel et al.

[Method for measurement of shear-wave impedance in the MHz region for liquid samples of approximately 1 ml](#)

F Eggers and T Funck

[A continuous wave transmission method for the ultrasonic spectrometry of liquids](#)

J Schultz and U Kaatze

[Acoustical absorption spectroscopy of liquids between 0.15 and 3000 MHz. I. High resolution ultrasonic resonator method](#)

U Kaatze, B Wehrmann and R Pottel

[Ultrasonic absorption and velocity measurements at mW peak power level in the range 50-500 MHz with variable pathlength cell](#)

V Uhlendorf, K -H Richmann and W Berger

[A high-easy-to-handle biconcave resonator for acoustic spectrometry of liquids](#)

R Polacek and U Kaatze

[Automatic ultrasonic velocimeter for liquids](#)

K Lautscham, F Wente, W Schrader et al.

# Ultrasonic resonator energy loss determination

F Eggers

Max-Planck-Institut für biophysikalische Chemie, D-3400 Göttingen,  
Federal Republic of Germany

Received 12 June 1989, in final form and accepted for publication 6 November 1989

**Abstract.** Ultrasonic resonators are used to study chemical kinetics in liquids (relaxation spectrometry). Resonator loss, proportional to  $Q^{-1}$ , is frequently determined from half-power bandwidth (amplitude 3 dB down from peak value); but other methods, in particular those utilising the phase characteristic at resonance, are often advantageous. This article describes three different techniques, employing (i) an AM driving signal for the resonator network, affecting the modulation envelope; (ii) a resonance peak compensation (RF amplitude and phase of the output signal); (iii) the phase slope (group delay) of the output signal. Relations for the one-dimensional ultrasonic resonator, circuit diagrams and measurement examples are given.

## 1. Introduction

Ultrasonic resonators are used for absorption and velocity measurements, especially on liquids in the 0.01–30 MHz frequency range; such data are important for studies in chemical relaxation spectrometry (Eigen and De Maeyer 1963, Stuehr 1986). Common applications of high precision ultrasonic resonators (USR) also occur in frequency control, temperature measurement and quartz microbalance techniques.

For investigations in chemical kinetics by means of broad band absorption measurements in liquids, resonator cells with two X-cut quartz transducers (input and output), enclosing the cylindrical cavity for a millilitre sample, have been developed in this laboratory (Eggers 1967, Eggers and Funck 1973, Eggers *et al* 1976); they are mostly employed for  $Q$ -determination from the half-power bandwidth (HPB) with a 3 dB amplitude drop from the resonance peak value. The general definition of resonator quality factor  $Q$  is  $2\pi$  (energy stored)/(energy dissipated per cycle). This method has often been described in the literature and will not be discussed in detail here. Special problems with respect to frequency stability arise for high  $Q$  resonators ( $Q > 10\,000$ ); in this case decay time measurements can be advantageous (Edmonds and Lamb 1958, Eggers and Richmann 1976).

Conventional HPB measurements suffer from certain disturbances, such as spurious mode propagation in the cavity with concomitant 'satellite' peaks (Colclough 1970, Del Grosso 1971), also from overlapping peaks at high liquid attenuation; they make 3 dB measurements inaccurate or impossible and require modified and improved techniques. Furthermore, slight temperature shift and oscillations can cause systematic errors if the HPB measure-

ment is too slow, i.e. if frequencies are not stable during a measurement cycle.

In the latter case accuracy can be improved with an amplitude modulation technique described in § 3, which obtains bandwidth values directly. Distorted (e.g. from satellites) and overlapping peaks can be evaluated with procedures utilising the *phase* response at resonance, performing a 'peak' measurement and putting less weight on the peak flanks. Finally, phase slope will be shown to be an effective parameter for resonator loss determination. Descriptions are given in §§ 4 and 5.

So far, phase measurements have been used only occasionally in ultrasonics; now, commercial vector voltmeters and network analysers open new possibilities for ultrasonic loss measurements (Eggers 1987).

## 2. Transfer function of plane wave ultrasonic resonator

The output of a simplified USR (one-dimensional wave propagation along coordinate  $x$ ; diffraction neglected; pressure reflection factor at liquid/transducer interfaces  $r^*$ ) as a function of angular frequency  $\omega$  and attenuation  $\alpha$  (neper/m) can be derived from a summation of partial waves  $\{\exp(i\omega t)[r^*\exp(-\alpha - i\omega/c)x]^{(2m-1)}\}$  (over  $m = 1, 2, 3, \dots$ ) or directly from the acoustic line equations (Meyer and Neumann 1979). Omitting the time factor  $\exp(i\omega t)$ , the complex output pressure  $p^*$  for an *ideal* USR ( $r^* = 1$ ) with the normalised frequency  $z = \omega/2f_0 = \pi f/f_0$  is

$$p^* = p_0 \frac{\sinh \alpha x \cos z - i \cosh \alpha x \sin z}{(\sinh \alpha x)^2 + (\sin z)^2} \quad (1)$$

with the magnitude

$$p = p_0 / [(\sinh \alpha x)^2 + (\sin z)^2]^{1/2} \quad (2)$$

and the phase (tangent and angle)

$$\tan \phi = -\coth \alpha x \tan z \quad (3)$$

$$\phi = -\tan^{-1}(\coth \alpha x \tan z) \quad (4)$$

where  $p_0$  is the input excitation amplitude,  $x$  the transducer distance (fluid column length),  $f_0 = c/2x$  is the column fundamental frequency and  $c$  is the sound velocity in the fluid.

Simple relations exist for the amplitudes at the multiple resonance (R) and antiresonance (A) frequencies  $f_n^R = n f_0$  and  $f_n^A = (n - \frac{1}{2}) f_0$  respectively ( $n = 1, 2, 3, \dots$  harmonic numbers) with  $\sin z_n^R = 0$  and  $\sin z_n^A = \pm 1$

$$p^R = \frac{p_0}{\sinh \alpha x} \quad (5)$$

$$p^A = \frac{p_0}{\cosh \alpha x} \quad (6)$$

Equations (5) and (6) permit attenuation measurements to be made for higher ( $\alpha x$ ) in a resonator with variable transducer distance  $x$ . Attenuation is obtained from the ratio  $p^A/p^R$ , eliminating  $p_0$  (Musa 1958, Cerf 1963, Eggers and Richmann 1989). It is essential to drive the input transducer with constant voltage from a low impedance source, since the electrical impedance changes during  $x$  variation; another possibility is to perform a ratio measurement for the output to input voltage. This condition must be obeyed for all HPB measurements if electrical input impedance varies with frequency; the same holds for transducer impedance measurements with a bridge, which should have a reference branch for voltage sampling at the transducer port (Eggers and Funck 1987).

For imperfect reflection ( $|r^*| < 1$ ) at the liquid/transducer interfaces the attenuation term generally becomes  $(\alpha x - \ln |r^*|)$  instead of  $(\alpha x)$ . Perfect reflection,  $|r^*| = 1$ , but with a phase angle, as it occurs for quartz transducers with air backing, shifts the eigenfrequencies of the fluid column, but does not increase the energy loss; this can be accounted for by introducing the frequency deviation from resonance  $\delta f \equiv f - f^R$ .

In the case of low attenuation ( $\alpha x \ll 1$ ) and close to a peak frequency ( $|\delta f| \ll f_0$ ) equations (2) and (3) can be linearised; the magnitude  $p$  and the phase  $\phi$  of a Lorentzian peak are

$$p \approx p_0 / [(\alpha x)^2 + (\pi \delta f / f_0)^2]^{1/2} \quad (7)$$

$$\tan \phi \approx -\frac{\pi \delta f}{\alpha x f_0} = -\frac{2\pi \delta f}{\alpha c} = -\frac{2\pi \delta f}{\alpha \lambda f_n^R} \quad (8)$$

and the  $Q$  factor for the ideal resonator is

$$Q = \frac{\pi}{\alpha \lambda} = \frac{\pi f}{2 f_0 \alpha x} = \frac{f}{\Delta f} \quad (9)$$

where  $\alpha \lambda$  is the liquid absorption per wavelength,  $\Delta f$  the half-power bandwidth.

### 3. Amplitude modulation method

The USR resembles a narrow-band electric filter, often a comb filter with multiple resonances. When an amplitude-modulated RF signal with the carrier frequency coinciding with a USR peak frequency is applied to the USR (network), its signal side-bands are more attenuated than the carrier, if the modulation frequency  $f_m$  is comparable to or in excess of  $\Delta f/2$ , resulting in a reduction of the modulation index  $M$  ( $M$  is the quotient of modulation to RF carrier amplitude). The phase shift of the modulation envelope also depends on the resonator  $Q$ . This method is used for microwave resonator  $Q$  measurements (Groll 1969).

A short calculation shows that for  $f_m = \Delta f/2$  the modulation index  $M$  is reduced by a factor  $\sqrt{2}$ , and the modulation envelope phase shift is  $-\pi/4$ . For such measurements it is important to use a small modulation index ( $M \approx 0.01$ ) for the input and to have linear demodulation of the output RF signal.

Figure 1 shows a block diagram of the circuit. The RF bridge incorporates the two-pole quartz into a four-pole network, exhibiting the series resonance of the quartz. The USR is driven from a modulated level measuring set (Wandel & Goltermann PSM-5), which also amplifies and detects the output signal. The modulating signal (frequency range  $f_m = 20-520$  Hz) is supplied by a network analyser (Hewlett-Packard 3577A), which displays the amplitude and phase of the modulation envelope as a function of  $f_m$ . Figure 2 demonstrates this method on an AT-cut shear quartz with water load at 6 MHz (Eggers and Funck 1987). The diagram also shows reference curves (broken curves) for modulation amplitude and phase from a signal passing a broad band attenuator without delay; the amplitude and phase reference curves are determined by the RF filter in the selective level meter. From the diagram (modulation amplitude and phase)  $\Delta f \approx 725$  Hz can be determined;  $f_m$  can be measured with a low frequency counter. This method is suited for high- $Q$  resonators; sensitivity might be enhanced by lock-in amplification after detection of the modulation signal ( $f_m$ ).

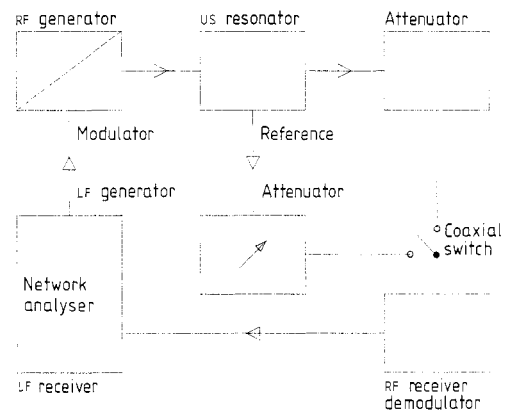
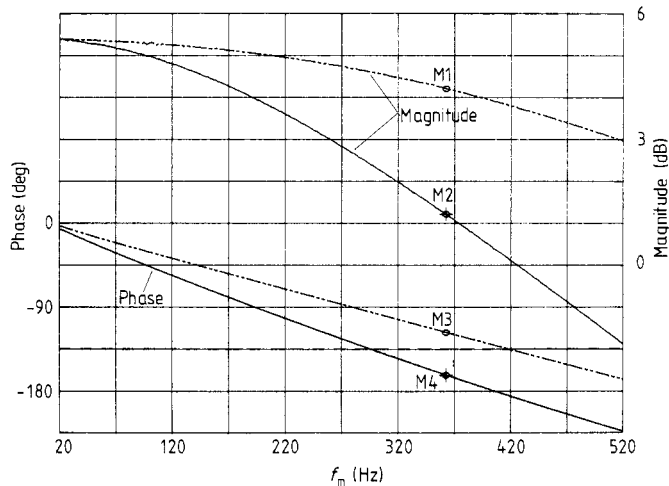


Figure 1. Block diagram for the amplitude modulation method. Reference attenuator (with step and fine adjustment) is set for equal amplitudes at the coaxial switch with unmodulated RF ( $M = 0$ ).



**Figure 2.** Network analyser measurement: modulation envelope magnitude (relative logarithmic scale) and phase of RF bridge output with water loaded AT shear quartz at  $f \approx 5982$  kHz. Modulation index  $M \approx 0.02$ . Broken curves: modulation magnitude and phase of reference signal through broad band attenuator. HPB determined from magnitude and phase is  $f \approx 725$  Hz. Markers (M1–M4) at  $f_m = 362.5$  Hz represent magnitudes of A/R of 4.21 dB (at M1) and 1.22 dB (at M2) and phases of A/R of  $-117.01^\circ$  (at M3) and  $-162.38^\circ$  (at M4).

#### 4. Peak vector compensation

This method utilises the phase characteristic of resonance peaks, but does not need a phase meter. The principle is to compensate the USR output at resonance to zero with an added constant RF signal (same frequency) by means of an adjustable bridge network (amplitude and phase). Following equations (1) and (5) the compensated complex signal (setting  $u^*$  for voltage instead of  $p^*$ ) is

$$u_c^* = u_0 \left( \frac{\sinh \alpha x \cos z - i \cosh \alpha x \sin z}{(\sinh \alpha x)^2 + (\sin z)^2} - \frac{1}{\sinh \alpha x} \right). \quad (10)$$

For small attenuation, equation (10) can also be linearised near resonance, resulting in the magnitude and phase for the balanced signal

$$u_c \approx \frac{u_0}{\sinh \alpha x} \frac{2\delta f}{\Delta f} \left[ 1 + \left( \frac{2\delta f}{\Delta f} \right)^2 \right]^{-1/2} \quad (11)$$

$$\phi_c \approx \pm \frac{\pi}{2} - \tan^{-1} \left( \frac{2\delta f}{\Delta f} \right) \quad (12)$$

which permit an evaluation of  $\Delta f$  in the peak (top) region, where normal amplitude variations are inadequate for  $Q$  determination, but the steepest phase changes occur. The circuit is shown in figure 3, together with a vector diagram for the (linearised) signal vector sum near resonance. While the locus for the uncompensated  $u$ -vector is a circle, the same is true for the  $u_c$ -vector, but with zero amplitude at resonance and the phase jumping from  $+\pi/2$  to  $-\pi/2$ .

An example is shown in figure 4 for a 7.6 MHz quartz in a bridge network. The uncompensated USR output signal is shown in broken curves. If the frequency sweep span is reduced,  $\Delta f \approx 137$  Hz can be obtained from the

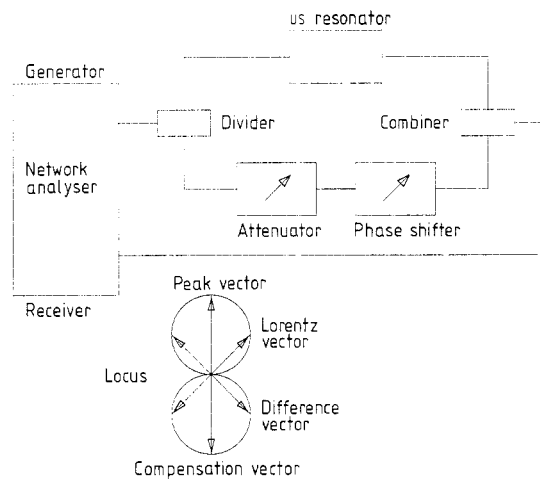


**Figure 3.** Block diagram for peak vector compensation and locus vector sum near resonance. The Lorentz vector,  $u^*$ , is obtained from equations (7) and (8) and the difference vector,  $u_c^*$ , is obtained from equations (11) and (12).

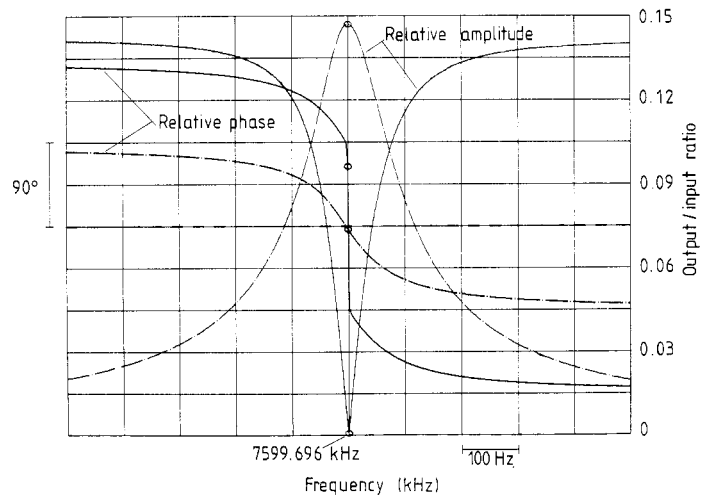


**Figure 4.** Output/input ratio (amplitude and phase) against frequency of 7.6 MHz quartz (Wuttke FT 243) in bridge network with balanced transformer MCL T1-6T. Broken curves: uncompensated bridge signal (amplitude and phase); full curves: RF-compensated signal. Ratio measurement made using network analyser Hewlett–Packard 3577 A. At the markers (open circles), the magnitude of A/R is  $811.2 \times 10^{-6}$  and its phase  $-6.13^\circ$ .

slope of  $u_c$  against  $f$  in accordance with the HPB method. The peak vector compensation is not limited to low attenuation cases but can be used also on ‘broad’ peaks with  $\alpha x > 0.1$ . Another advantage is that eventual electrical feedthrough, as may occur at higher frequencies, can be simultaneously compensated in the same circuit.

#### 5. Phase measurements

So far, phase measurements have been applied to USR work only in a few cases (Colclough 1973, Sarvazyan and Zaretskii 1982, Eggers 1987) and are more often applied

in audio frequency acoustics. This may change with the availability of high sensitivity (superheterodyne type) RF phasemeters as vector voltmeters and network analysers; such devices permit swept operation too, with high frequency resolution and convenient measurement routines. The phase against frequency characteristic of a USR reflects  $Q$  as well as the associated amplitude spectrum. Since the phase is defined by  $\tan \phi = \text{Im}(u^*)/\text{Re}(u^*)$ , eliminating the denominator in equation (1), relations are simpler than for amplitude (with squaring operations). Equation (3) shows that for a pure mode peak,  $\tan \phi$  against  $\tan z$  is a straight line with slope  $s = -\coth \alpha x$ ; close to resonance  $\tan \phi$  against  $f$  is approximated by a straight line with slope  $s' = -\pi/(f_0 \alpha x)$ . Some phase meters display the group delay time  $\tau$ , which is proportional to the phase slope (Zinke and Brunswig 1986).

Group delay time, defined in equation (13), is calculated from equation (4)

$$\tau \equiv -\frac{1}{2\pi} \frac{d\phi}{df} = \left\{ 2f_0 \tanh \alpha x \left[ 1 + \left( \frac{\sin z}{\sinh \alpha x} \right)^2 \right] \right\}^{-1} \quad (13)$$

The resonance and antiresonance values of group delay time are

$$\tau^R = \frac{1}{2f_0 \tanh \alpha x} \quad (14)$$

$$\tau^A = \frac{\tanh \alpha x}{2f_0} \quad (15)$$

For low attenuation ( $\alpha x \ll 1$ ), linearisation results in

$$\tau^R \approx \frac{1}{2f_0 \alpha x} \quad (16)$$

$$\tau^A \approx \frac{\alpha x}{2f_0} \quad (17)$$

and

$$\Delta f \approx \frac{1}{\pi \tau^R} \quad (18)$$

Another useful relation, including imperfect reflection, is

$$\alpha x - \ln |r^*| = \tanh^{-1} \sqrt{\tau^A/\tau^R} \quad (19)$$

From measurements with a variable transducer distance cell,  $\alpha$  and  $|r^*|$  can be separated by linear regression of  $\tanh^{-1} \sqrt{\tau^A/\tau^R}$  against distance  $x$ .

Attenuation can also be determined from the difference  $\Delta\tau = \tau^R - \tau^A$ :

$$\alpha x - \ln |r^*| = \frac{1}{2} \sinh^{-1} (1/f_0 \Delta\tau) \approx 1/2f_0 \Delta\tau \quad (20)$$

Phase meters determine phase slope from finite frequency increments (delay aperture, which is adjustable in most devices). Increased aperture reduces phase slope fluctuations and permits improved resolution. If the difference quotient for a finite aperture  $2\delta f$  is calculated from equation (4), instead of the differential quotient in equation (13), one gets for the finite aperture delay time

at resonance  $t^R$

$$t^R = -\frac{1}{2\pi} \frac{\phi(+\delta f) - \phi(-\delta f)}{2\delta f} = \frac{1}{2\pi\delta f} \tan^{-1} \left[ \coth \alpha x \tan \left( \pi \frac{\delta f}{f_0} \right) \right] \quad (21)$$

Since for practical measurements  $\delta f/f_0 \ll 1$ , the tangent in equation (21) can be substituted by the argument without significant error; now equation (14) is used to establish a relation between  $t^R$  and  $\tau^R$

$$\tau^R \approx \frac{\tan(2\pi\delta f t^R)}{2\pi\delta f} \quad (22)$$

Finite aperture group delay times  $t^R$  measured with larger apertures for 'noise' reduction (smoothing) can easily be corrected through equation (22).

As an example figure 5 shows the transfer function (ratio measurement) and the group delay for a dry AT quartz (unloaded) in a bridge as in figure 2; from the maximum  $\tau^R$  and also the amplitude one finds  $\Delta f \approx 54$  Hz. Figure 6 gives  $\tau$  for a water-filled USR ( $x \approx 4.9$  mm) near 95.5 MHz ( $\alpha x \approx 1.0$ ) together with the output amplitude (ratio measurement); any HPB ( $-3$  dB) measurement would be impossible in this case. This measurement indicates that the total attenuation at 95 MHz is dominated by the water absorption. The separation of  $\alpha$  and  $|r^*|$  could be obtained by a variation of  $x$ , or by a calibration measurement with a reference liquid. The baseline elevation ('bump') in this diagram is from the vicinity of the 19th quartz harmonic; its influence can be eliminated by measurement of both  $\tau^R$  and  $\tau^A$  and application of equations (19) or (20).

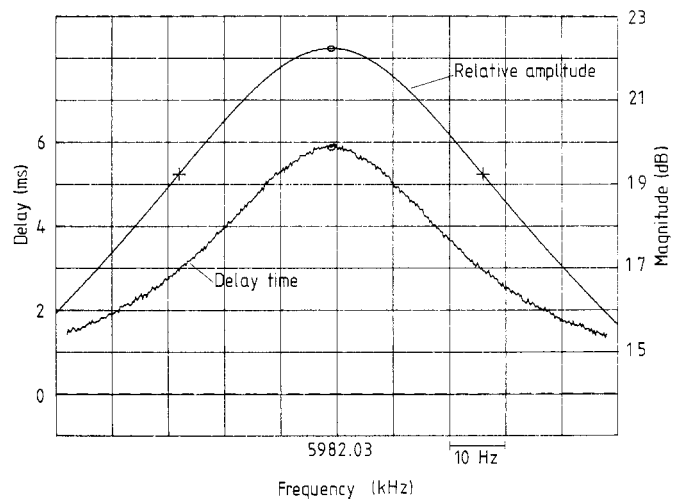


**Figure 5.** Amplitude ratio (A/R: output/reference) and group delay time  $\tau$  of RF-bridge output with air loaded (dry) AT shear quartz against frequency near 5982 kHz. Delay aperture 4 Hz. HPB from amplitude and group delay is  $\Delta f \approx 54$  Hz. Measurements made with network analyser Hewlett-Packard 3577 A. Markers at 5982.029 kHz (○) indicate magnitude and delay values of A/R at 22.23 dB and 5.87 ms respectively. Markers at the offset frequency  $\pm 27$  Hz (+; left  $-27$  Hz, right  $+27$  Hz) show magnitudes (A/R) of  $-2.99$  dB (left) and  $-3.00$  dB (right).

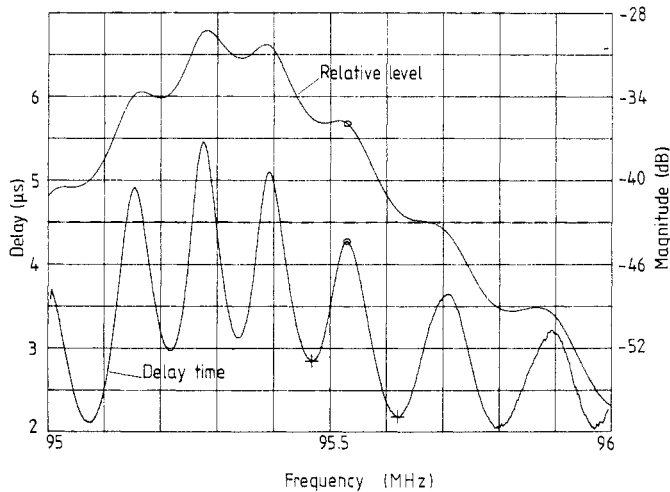


**Figure 6.** Amplitude ratio ( $A/R$ : output/input) and group delay time  $\tau$  of water-filled ultrasonic resonator cell between 95 MHz and 96 MHz; quartz distance  $x \approx 4.9$  mm,  $\alpha x \approx 1.0$ ; delay aperture 10 kHz. Feed-through has been compensated with a circuit similar to figure 3, employing an adjustable Wayne Kerr VHF admittance bridge B 801 B. Network analyser: Hewlett-Packard 3577 A. Markers at 95.53 MHz ( $\circ$ ) occur at a magnitude of  $-35.95$  dB and delay  $4.28 \mu\text{s}$ . At 95.47 MHz ( $+$ ) the delay is  $2.85 \mu\text{s}$ ; at 95.62 MHz ( $+$ ) the delay is  $2.19 \mu\text{s}$ .

## 6. Conclusions

Among the methods discussed in this article, HPB measurements are appropriate only for 'pure' Lorentzian peaks without satellites (the latter not occurring in a one-dimensional USR) and neighbouring peak interference. A frequency-lock circuit helps to achieve a semiautomatic frequency shift to the 3 dB points (Thein and Eggers 1980). Other dB values, non-symmetric bandwidth or inflection point (Leisure 1972) measurements, following equation (7) for  $Q$  calculation, have been suggested. Decay time measurements also suffer from spurious modes, which cause multiexponential decay curves. For the AM method, limitations are analogous to the HPB method, but peak evaluation might be faster and less dependent on drift. In addition, the AM method requires a receiver bandwidth covering the signal sidebands; this may limit the AM method to smaller  $\Delta f$  values.

Peak vector compensation is less 'satellite affected', since the measurement region is only on the top, where the amplitude ratio between main peak and spurious peak is better than on the flank. The straight line characteristic near resonance, as seen in figure 4, permits a judgement of peak perturbation. On the other hand this technique is rather elaborate and needs a high resolution RF-compensation circuit (continuous RF-attenuator and phase shifter, or a precision-type RF bridge).

The most promising method now appears to be direct phase measurement, especially with the new vector voltmeters or network analysers. For modern instruments, phase measurements are virtually amplitude independent over a wide range, but phase 'standards' are highly desirable for calibration, especially broad band ones for  $\pm \pi/4$ , corresponding to the 3 dB points. A PLL circuit,

including a vector voltmeter (Rohde & Schwarz ZPU), has been built in this laboratory, which pulls the generator frequency of a modified level meter (Wandel & Goltermann SPM-16) to both HPB points of a USR. This circuit appears to have higher stability than the frequency-lock mentioned above, which uses amplitude response. Phase measurements appear to have better chances than amplitude measurements for the discrimination and computer separation of interfering modes, i.e. the calculation of the main peak half-power bandwidth, independent of vicinal satellites. Only simple mathematical operations are needed to obtain  $\tan \phi = \text{Im}(u^*)/\text{Re}(u^*)$ ; this holds also for the (vector!) superposition of adjacent peaks (including satellites), in contrast to the magnitude of added vectors, as can be realised by a summation of different complex functions like equation (1). Modern network analysers determine  $\text{Re}(u^*)$  and  $\text{Im}(u^*)$  separately; it is possible to calculate and display  $\tan \phi$  'on line', judge the purity of the mode directly and obtain  $\alpha x$  by a regression program;  $\tan \phi$  appears to be better suited for USR evaluation than the angle  $\phi$  itself. Further chances exist through phase slope techniques, which can resolve resonator parameters not obtainable with amplitude measurements. These questions will be discussed in a later publication. Nearly all the techniques mentioned here can also be applied to electrical (non-acoustic) resonant circuits.

## Acknowledgments

I want to thank Dr Th Funck for valuable discussions and suggestions and Ms G Schäfer for patient and careful typing work.

## References

- Cerf R 1963 Sur l'interféromètre ultrasonore à deux transducteurs et la spectroscopie à fréquence continûment variable *Acustica* **13** 417-21
- Colclough A R 1970 Higher modes in acoustic interferometry *Acustica* **23** 93-9
- 1973 Systematic errors in primary acoustic thermometry in the range 2-20 K *Metrologia* **9** 75-98
- Del Grosso V A 1971 Analysis of multimode acoustic propagation in liquid cylinders with realistic boundary conditions—application to sound speed and absorption measurements *Acustica* **24** 299-311
- Edmonds P D and Lamb J 1958 A method for deriving the acoustic absorption coefficient of gases from measurement of the decay-time of a resonator *Proc. Phys. Soc.* **71** 17-32
- Eggers F 1967 Eine Resonatormethode zur Bestimmung von Schall-Geschwindigkeit und Dämpfung an geringen Flüssigkeitsmengen *Acustica* **19** 323-9
- 1987 Güte-Meßverfahren für Ultraschall-Resonatoren *Fortschritte der Akustik-DAGA '87 (Aachen)* pp 413-6
- Eggers F and Funck Th 1973 Ultrasonic measurements with milliliter liquid samples in the 0.5-100 MHz range *Rev. Sci. Instrum.* **44** 969-77
- 1987 Method for measurement of shear-wave impedance in the MHz-region for liquid samples of  $\sim 1$  ml *J. Phys. E: Sci. Instrum.* **20** 523-30

- Eggers F, Funck Th and Richmann K-H 1976 High  $Q$  ultrasonic liquid resonators with concave transducers *Rev. Sci. Instrum.* **47** 361–7
- Eggers F and Richmann K-H 1976 Decay time measurement for high- $Q$  ultrasonic resonators *Rev. Sci. Instrum.* **47** 378–9
- 1989 Ultraschall-Dämpfungsmessungen mit einem Resonator variabler Länge *Fortschritte der Akustik-DAGA '89 (Duisburg)* pp 247–50
- Eigen M and De Maeyer L 1963 Relaxation methods *Techniques of Organic Chemistry* (ed A Weissberger) Vol. VIII Part II (New York: Interscience)
- Groll H 1969 *Mikrowellenmeßtechnik* (Braunschweig: Vieweg) pp 314–6
- Leisure R G 1972 An improved cw technique for measurement of ultrasonic attenuation *Rev. Sci. Instrum.* **43** 1021–3
- Meyer E and Neumann E-G 1979 *Physikalische und Technische Akustik* (3rd edn) (Braunschweig: Vieweg) p 40 ff
- Musa R S 1958 Two-crystal interferometric method for measuring ultrasonic absorption coefficients in liquids *J. Acoust. Soc. Am.* **30** 215–9
- Sarvazyan A P and Zaretskii A A 1982 Device for measuring the characteristic of acoustic resonators *Measurement Techniques USSR* **25** 91–4 (translated from *Izmeritel'naya Tekhnika*)
- Stuehr J E 1986 Ultrasonic methods *Techniques of Chemistry: Investigations of Rates and Mechanisms of Reactions* ed C F Bernasconi (4th edn) Vol. VI Part II (New York: Wiley-Interscience)
- Thein S and Eggers F 1980 Semiautomatic control circuit for level measuring set *Internal Technical Report* Max-Planck-Institut für biophysikalische Chemie, Göttingen
- Zinke O and Brunswig H 1986 *Lehrbuch der Hochfrequenztechnik Band I (Hochfrequenzfilter, Leitungen, Antennen)* (3rd edn) (Berlin: Springer)